

# Optimization Methods Evaluation for the Design of Radial Flux Surface PMSM

Yannis L. Karnavas, Christos D. Korkas

**\*Abstract** -- Conventional high torque low speed drive systems commonly have a mechanical transmission between the induction motor and the load consisting of gears, gear heads, belt/pulleys or camshafts. The main drawbacks of such setups, are the deficiency of the drive system, its high cost and the maintenance needs. An alternative to this, is the replacement of the induction motor and its mechanical transmission elements with a permanent magnet (PM) synchronous motor (PMSM) directly coupled to the load running at low speed. In this context, the paper deals with the design evaluation of a 5kW 50rpm motor and concentrates on two radial flux promising topologies i.e. with surface-mounted permanent magnets with inner and outer rotor. Since the goal is mainly the minimization of the machine's active weight (with respect to constraints related to outer dimensions, efficiency and cost), the designs of the PM machines are conducted by solving an optimization problem. Three optimization methods are adopted and three weighted cost functions are presented. The effectiveness of the methods in finding competitive alternative PMSM designs is then evaluated. The presented results are compared with other found in literature and reveal satisfactorily enhanced design solutions and performance of the proposed methods.

**Index Terms**—Permanent magnet synchronous motor, electrical machine design, optimization algorithms, low speed applications.

## I. INTRODUCTION

NOWADAYS, induction motors are used in very large numbers in industry and account for approximately 65% of the worldwide energy consumption. As environmental concern increases in one hand and economy plays an important role on the other, electrical drives with higher efficiency and lower costs are desirable [1]. Thus, the replacement of induction machines with PMSM can be an attractive alternative due to several reasons: a) PMSM are capable of producing very high starting torque, b) current drawn by PMSM is directly proportional to torque so the latter can be calibrated directly from current reading -this is not possible with induction motor-, c) The gearbox can be eliminated in low speeds i.e. lower than 500rpm, d) PMSM have higher efficiency -no rotor winding resulting in lower copper losses-, e) considerable savings in power consumption and lower noise pollution, f) relatively low price of the magnetic materials used.

It is known that low (or high) speed drives without a gearbox are called direct drives. Common low-speed direct drives applications in which PM machines are used, include wind turbines, boat propulsion, elevators, and waste water

treatment plants. Direct drives for wind turbine generators are widely studied i.e. [2]-[4]. A boat propulsion system consisting of 100kW PMSM is designed and analyzed in [5]. An axial flux PM machine for elevator system has been studied in [6], while PMSM for waste water direct-drive mixer motor is thoroughly discussed in [7], [8].

The paper aims to present the effectiveness of certain optimization algorithms in finding competitive alternative radial flux surface PMSM designs to be used as replacements of traditional induction motor-gearbox low speed drive systems. The relative topologies and the design procedure are presented first and the three optimization algorithms adopted are described secondly. Following these, a categorization of the design variables, the constant quantities and the relevant constraints is being done and the proposed cost functions adopted are presented. The corresponded analytical optimization results are shown next and compared with those found in literature.

## II. RADIAL FLUX PMSM UNDER EXAMINATION

Radial flux's PMSM are quite conventional PM machines and they are widely used for direct-driven applications. In these machines, the flux flows radially inside the machines while the current flows in the axial direction. Fig. 1 shows the cross sections of the configurations under study here: a) the surface mounted PM (SMPM) motor with inner rotor and b) the SMPM motor with outer rotor. In the first configuration, the permanent magnets are placed on the rotor surface as shown in Fig. 1(a), while in the second configuration, the permanent magnets are placed along the inner circumference of the rotor (outer part), therefore a stationary wound stator is located in the centre of the machine as shown in Fig. 1(b). Both configurations have advantages and disadvantages but -up to now- the first one seems to be the most preferable. Fig. 2 shows the general geometry of a PMSM regarding the magnet length ( $l_m$ ), the pole angle ( $\alpha$ ), the airgap length ( $\delta$ ), the inner stator diameter ( $D_s$ ), the rotor diameter ( $D_r$ ) and the outer diameter of the machine ( $D_o$ ).

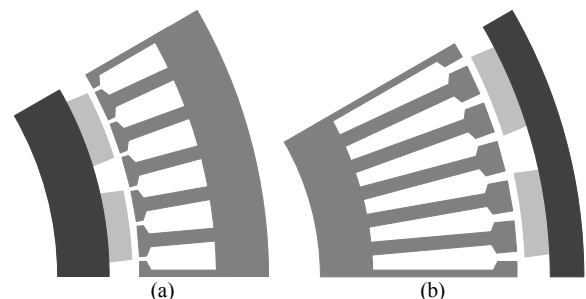


Fig 1. Surface-mounted PM motor's cross section (one pole pair), a) inner rotor configuration and b) outer rotor configuration.

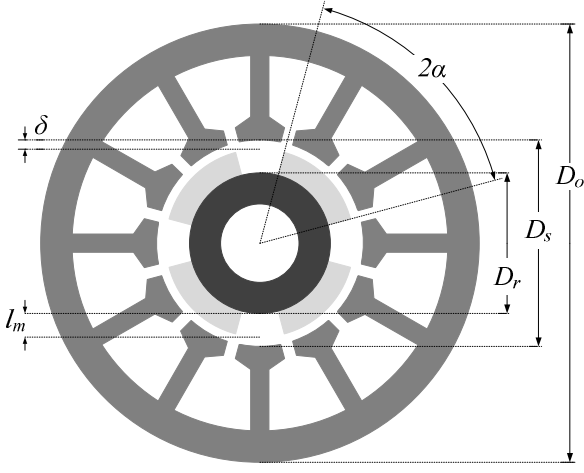


Fig 2. Generic geometrical parameters for the PMSM designs (cross section of a SMPM motor with inner rotor).

More detailed geometrical parameters for the two configurations are shown in Fig. 3. In this figure, the quantities  $b_{ss0}$ ,  $b_{ss1}$ ,  $b_{ss2}$  and  $b_{st}$  refer to stator slot widths (bores) while the quantities  $h_{sw}$ ,  $h_{ss}$ ,  $h_{sy}$  and  $h_{ry}$  refer to stator slot heights. The ratio of the stator slot opening to the slot width is defined as

$$k_{open} = \frac{b_{ss0}}{b_{ss1}} \quad (1)$$

Also, if we denote as  $Q_s$  the number of stator slots then the slot pitch  $\tau_s$  can be defined as,

$$\tau_s = \pi \frac{D_s}{Q_s} \quad (2)$$

#### A. Inner rotor SMPM motor topology

For the inner rotor configuration (Fig. 3(a)) the following equations can be derived:

$$D_s = D_r + 2l_m + 2\delta \quad (3)$$

$$b_{ss1} = \pi \frac{D_s + 2h_{sw}}{Q_s} - b_{st} \quad (4)$$

$$b_{ss2} = \pi \frac{D_s + 2h_{ss}}{Q_s} - b_{st} \quad (5)$$

$$h_{sy} = \frac{1}{2}(D_o - D_s - 2h_{ss}) \quad (6)$$

The slot area  $A_s$  is then given by,

$$A_s = \frac{1}{2}(b_{ss1} + b_{ss2})(h_{ss} - h_{sw}) \quad (7)$$

#### B. Outer rotor SMPM motor topology

Respectively, the following equations can be derived for the outer rotor configuration (Fig. 3(b)):

$$D_s = D_r - 2l_m - 2\delta \quad (8)$$

$$b_{ss1} = \pi \frac{D_s - 2h_{sw}}{Q_s} - b_{st} \quad (9)$$

$$b_{ss2} = \pi \frac{D_s - 2h_{ss}}{Q_s} - b_{st} \quad (10)$$

1

$$h_{ry} = \frac{1}{2}(D_o - D_r) \quad (12)$$

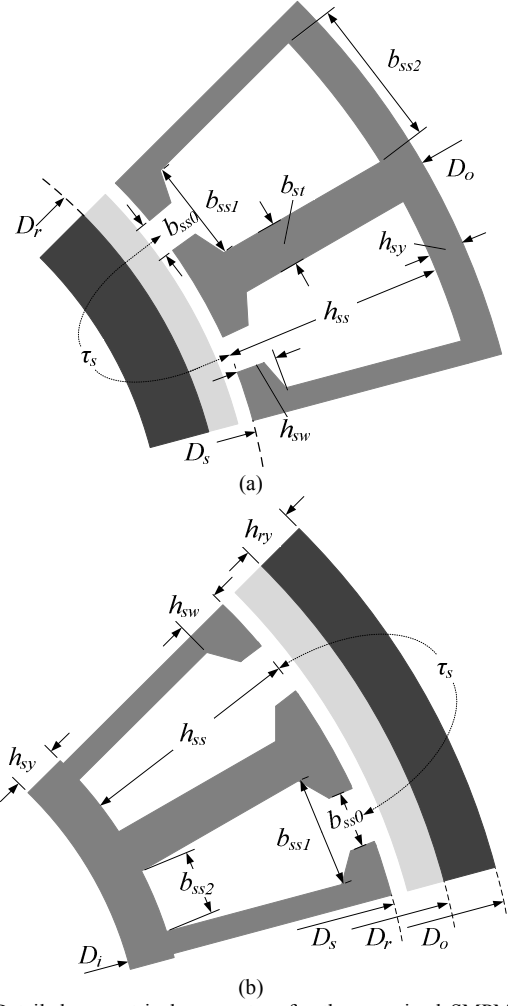


Fig 3. Detailed geometrical parameters for the examined SMPM motor designs, a) inner rotor configuration, b) outer rotor configuration.

For both configurations it should be noted that, since the inner stator diameter  $D_s$  is very large compared to the slot pitch  $\tau_s$ , the relevant slot widths (which are actually arcs of circles) are approximated as straight lines in Eqs.(4)-(5) and Eqs.(9)-(10) respectively.

#### C. Magnetic properties considerations of SMPM motor

Since the design procedure relies on the amplitude of the fundamental airgap flux density  $B_\delta$ , its calculation should be conducted. For SMPM motor designs the airgap flux density is assumed to have a rectangular shape (as wide as the magnet width) and a maximum value of  $B_m$ . Using the Carter factor [9],

$$k_C = \frac{\tau_s}{\tau_s - \frac{(k_{open} b_{ss1})^2}{k_{open} b_{ss1} + 5\delta}} \quad (13)$$

this value can be calculated [7]:

$$B_m = \frac{B_r k_{leak}}{1 + \frac{\mu_r \delta k_C}{l_m}} \quad (14)$$

where  $B_r$  is the remanence flux density of the magnet,  $k_{leak}$  the leakage factor (the percentage of the flux lines which pass through the airgap) and  $\mu_r$  the relative magnet

dependency on the poles number  $p$  can be used:

$$k_{leak} = \frac{100 - (7p/60 - c)}{100} \quad (15)$$

where  $c$  is 0.5 and 3.0 for inner rotor and outer rotor SMPM motors respectively, which are our cases.

#### D. Electrical properties considerations of SMPM motor

The electrical parameters of the SMPM under examination shall be defined next i.e. inductances, stator's per phase resistance, supply and induced voltages, ampere-turns and current density. Since this kind of motors are of a non salient type, the direct and quadrature axis synchronous inductances ( $L_d$ ,  $L_q$ ) w.r.t. the leakage inductance and the magnetizing reactances ( $L_l$ ,  $L_{md}$ ,  $L_{mq}$ ) are:

$$L_d = L_q = L_l + L_{md} = L_l + L_{mq} \quad (16)$$

where

$$L_l = pqn_s^2 L \mu_0 \lambda_l \quad (17)$$

$$L_{md} = \frac{3}{\pi} (qn_s k_{w1})^2 \frac{\mu_0}{\delta k_c + \frac{l_m}{\mu_r}} (D_s - \delta) L \quad (18)$$

and  $q$  is the number of slots per pole per phase,  $n_s$  is conductors per slot number,  $\lambda_l$  is the specific permeance coefficient of the slot opening depending on the slot geometry,  $k_{w1}$  is the fundamental winding factor (equal to unity for  $q=1$ ) and  $L$  is the active machine length [9].

The stator's winding per phase resistance can be evaluated as:

$$R = \frac{\rho_{Cu} n_s^2 q \{ pL + k_{ew} \pi (D_s + h_{ss}) \}}{f_s A_s} \quad (19)$$

where  $f_s$  is the slot fill factor equals to 0.45 for distributed windings and  $k_{ew}$  is the end-winding factor [10]. Consequently, the induced voltage's rms value is expressed,

$$E = \frac{1}{\sqrt{2}} \omega k_{w1} q n_s B_m L (D_s - \delta) \quad (20)$$

Finally, the ampere-turns are derived from the peak current loading,

$$n_s I = \frac{4T}{\pi (D_s - \delta)^2 L B_\delta k_{w1} k_{sl}} \tau_s \quad (21)$$

where  $k_{sl}$  is a slot leakage loss compensating factor which equals to 0.95 and 0.94 for inner and outer rotor configurations respectively. The current density is therefore given by,

$$J = \frac{n_s I}{A_s f_s} \quad (22)$$

The supply voltage across one phase can be derived using the corresponding vector diagram ( $I_q=I$ ),

$$V = \sqrt{(|E| + R|I_q|)^2 + (L_d \omega |I_q|)^2} \quad (23)$$

It should be noted that this voltage is actually the inverter's output voltage according to Fig. 4. For a bad scenario of 50% modulation ratio, the  $V_{LL}$  is about 30% of the rectified dc voltage across the capacitor. Thus,  $V$  is approximately taken as 86.55Volts.

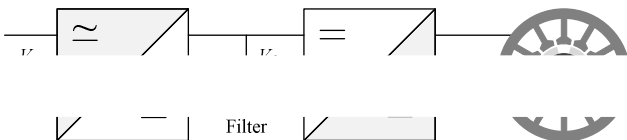


Fig 4. Typical PM motors drive setup.

#### E. Thermal considerations of SMPM motor

Generally, the thermal behavior of a motor depends on the heat sources (such as copper and iron losses) and on the motor's geometry. For PMSM, traditional techniques used include finite element analysis (FEA) and computational fluid dynamics (CFD). Another method is the analytical lumped circuit, which in terms of calculation speed has a clear advantage over the previous. Recently, more parameter sensitive techniques have been proposed i.e. [11]. A detailed thermal analysis is beyond the scope of this work, so the focus here will be concentrated on the slot current density calculation (Eq. 22) for each proposed geometry. Each value should not exceed the maximum allowable slot current density ( $J_{max}$ ). According to [12], for air-cooled machines, this value is about 800 A/cm<sup>2</sup>, while for forced cooling  $J_{max}$  is allowed to be more than 1kA/cm<sup>2</sup>.

### III. OPTIMIZATION METHODS USED

The aforementioned PMSM geometries designs under examination refer to a constrained optimization problem of the form

$$\min_x f(x) \text{ subject to } g(x) \leq 0, h(x) = 0 \quad (24)$$

where  $g(x)$  and  $h(x)$  are the inequalities and equalities constraint set respectively. In particular, the problem can be expressed as finding the minimum of a function specified by

$$\min f(x) \text{ such that } \begin{cases} c(x) \leq 0 \\ c^{eq}(x) = 0 \\ A \cdot x \leq b \\ A^{eq} \cdot x = b^{eq} \\ l^b \leq x \leq u^b \end{cases} \quad (25)$$

where  $b$ ,  $b^{eq}$ ,  $l^b$  and  $u^b$  are vectors,  $A$  and  $A^{eq}$  are matrices,  $c(x)$  and  $c^{eq}(x)$  are functions that return vectors, and  $f(x)$  is a function that returns a scalar. Finally,  $f(x)$ ,  $c(x)$ , and  $c^{eq}(x)$  can be (and in our case are) nonlinear functions. The optimization methods used here for solving our problem expressed in the form of Eq. (25) are briefly presented next.

#### A. Method 1: "Fmincon"

"Fmincon" is a constrained local non-linear programming (NLP) solver from MATLAB® optimization toolbox [13]. For such a problem like Eq. (25), the auxiliary Lagrangian function is:

$$L(x, \lambda) = f(x) + \sum \lambda_i c_i(x) + \sum \lambda_j c_j^{eq}(x) \quad (26)$$

where  $\lambda_i$  are Lagrange multipliers. "Fmincon" uses a Hessian (a square matrix of second-order partial derivatives of a function, which actually describes the local curvature of this multi-variable function) as an input which in case of Eq. (26) takes the form,

$$H = \nabla^2 L(x, \lambda) = \nabla^2 f(x) + \sum \lambda_i \nabla^2 c_i(x) + \sum \lambda_j \nabla^2 c_j^{eq}(x) \quad (27)$$

The "fmincon" algorithm may use four different mathematical solution packages namely: a) Active Set, b) SQP (this is usually used), c) Trust-region-reflective, d) interior-point. The first two of them do not accept a user-supplied Hessian but they compute a quasi-Newton

optimization, quasi-newton methods (a special case of variable metric methods) are algorithms for finding local

maxima and minima of functions. Quasi-Newton methods are based on Newton's method to find the stationary point of a function, where the gradient is 0. Newton's method assumes that the function can be locally approximated as a quadratic in the region around the optimum, and uses the first and second derivatives to find the stationary point. In higher dimensions, Newton's method uses the gradient and the Hessian matrix of second derivatives of the function to be minimized. In quasi-Newton methods the Hessian matrix does not need to be computed. The Hessian is updated by analyzing successive gradient vectors instead.

#### B. Method 2: Genetic Algorithm

A genetic algorithm (GA) is a well-known search heuristic that mimics the process of natural selection. This heuristic is routinely used to generate useful solutions to optimization and search problems. GA belong to the larger class of evolutionary algorithms, which generate solutions to optimization problems using techniques inspired by natural evolution, such as inheritance, mutation, selection, and crossover.

In a genetic algorithm, a population of candidate solutions (called individuals or phenotypes) to an optimization problem is evolved toward better solutions [14]. Each candidate solution has a set of properties (its chromosomes or genotype) which can be mutated and altered; traditionally, solutions are represented in binary as strings of 0's and 1's, but other encodings are also possible [15]. The evolution usually starts from a population of randomly generated individuals, and is an iterative process, with the population in each iteration called a generation. In each generation, the fitness of every individual in the population is evaluated; the fitness is usually the value of the objective function in the optimization problem being solved. The more fit individuals are stochastically selected from the current population, and each individual's genome is modified (recombined and possibly randomly mutated) to form a new generation. The new generation of candidate solutions is then used in the next iteration of the algorithm. Commonly, the algorithm terminates when either a maximum number of generations has been produced, or a satisfactory fitness level has been reached for the population.

#### C. Method 3: Pattern Search

This method performs a systematic direct search which generates and maintains multi-dimensional search directions in a dynamic manner. The following definitions make the underlying processes visual and clearer [16].

A set of values, one for each of the  $N$  as a point in an  $N$ -dimensional space point to the next is called a move. The process of going from one move to another where the objective function's value has been improved is called a success otherwise is a failure. Exploratory moves are made during the first, exploratory phase. Their success or failure provides some basic knowledge about the behavior of the objective function. One single coordinate value at a time is changed when the step size is added to or subtracted from

response function. The point at the end of this series of moves along one coordinate is the temper head. The head is defined by the coordinates of all successful exploratory moves. This in fact becomes the new base point. The pattern is the vector that connects one base point with the next. Pattern moves then replace exploratory moves. A pattern move starts from a newly established base point and duplicates the pattern leading to that base point (this also generates a new temper head). The heuristic used here is that whatever constituted a successful set of moves in the past is likely to prove successful again in the future.

### IV. PROBLEM DATA CATEGORIZATION & OPTIMIZATION RESULTS

From the previous three paragraphs, PMSM design problem data, relevant constraints, objective functions and solution methods particularities should be carefully chosen and taken into account. Since the goal of this evaluation study is to define suitable PMSM as replacements of a real world's "induction motor-gearbox" system and at the same time to be able to compare our results with other found in literature, a 5kW, 50rpm waste-water treatment plant mixer motor is chosen [17]. Its operating characteristics (corresponding desired PMSM characteristics) are shown in Appendix (Table XVI). Due to the large number of variable names, symbols etc., all info as well as the results obtained will be presented here in a tabularized form.

#### A. Design Variables, Constants and Problem Constraints

Combining Figs. 2-3 and Eqs. (1)-(23), there are twelve design variables that are needed to be computed (optimized) by the algorithms. The other quantities can be calculated through these values. Table XVII in the Appendix, shows these design variables, all of them related to the motor's geometry. In the same Table the upper and lower bounds of the variables are given. Additionally, Table XVIII summarizes the constant values used in the calculations, while Table XIX gather the required problem constraints.

#### B. Cost (Objective) Functions and Case Studies

The main concern of the PMSM design can involve many quantities. In this context, a simple formulation for the objective (cost) function to be minimized is adopted:

$$CF_j = \beta_i \cdot Q_i \quad (28)$$

where  $\beta_i$  is a  $1 \times i$  row matrix containing the cost function's weight coefficients and  $Q_i$  is a  $i \times 1$  column matrix containing the quantities under concern. It can be seen that this type of formulation can be expanded easily. Here, the quantities chosen are the total machine weight, the total magnets weight and the total copper losses ( $i=3$ ). Furthermore, although numerous cost functions can be produced that way, three variations ( $j=3$ ) are examined here:

$$\begin{aligned} CF_1 &= [0.70 \quad 0.15 \quad 0.15] \cdot [M_w^{tot} \quad P_L^{tot} \quad M_m^{tot}]^T \\ CF_2 &= [0.15 \quad 0.70 \quad 0.15] \cdot [M_w^{tot} \quad P_L^{tot} \quad M_m^{tot}]^T \end{aligned} \quad (29)$$

Such step is then repeated in the same direction as many times as it produces an improvement (increase) in the

TABLE I  
DESIGN VARIABLES RESULTS THROUGH **FMINCON** OPTIMIZATION  
METHOD FOR INNER ROTOR GEOMETRY

	$CF_1$	$CF_2$	$CF_3$
$N_m$	60	62	32
$N_{spp}$	0.48	0.50	0.38
$D_o$ (cm)	25.63	28.25	37.60
$D_{rc}$ (cm)	20.00	20.00	21.50
$L$ (cm)	10.80	10.00	15.60
$n_s$	14	10	13
$l_m$ (mm)	8.35	15.00	15.00
$b_{ts}$ (mm)	4.05	2.50	8.20
$h_{ss}$ (mm)	9.20	15.50	41.70
$h_{sw}$ (mm)	2.00	2.50	13.00
$k_{open}$	0.49	0.357	0.20
$\delta$ (mm)	3.0	3.0	3.0

TABLE II  
DESIGN VARIABLES RESULTS THROUGH **GA** OPTIMIZATION METHOD FOR  
INNER ROTOR GEOMETRY

	$CF_1$	$CF_2$	$CF_3$
$N_m$	72	60	20
$N_{spp}$	0.56	0.2332	0.9992
$D_o$ (cm)	24.41	28.74	37.66
$D_{rc}$ (cm)	20.00	20.24	26.15
$L$ (cm)	10.00	11.79	10.01
$n_s$	11	10	20
$l_m$ (mm)	7.50	7.40	10.50
$b_{ts}$ (mm)	2.50	9.70	8.60
$h_{ss}$ (mm)	9.00	21.40	22.10
$h_{sw}$ (mm)	2.00	4.80	5.00
$k_{open}$	0.6089	0.8020	0.2361
$\delta$ (mm)	3.0	3.0	13.9

TABLE III  
DESIGN VARIABLES RESULTS THROUGH **PS** OPTIMIZATION METHOD FOR  
INNER ROTOR GEOMETRY

	$CF_1$	$CF_2$	$CF_3$
$N_m$	60	62	36
$N_{spp}$	0.7427	0.2881	0.48
$D_o$ (cm)	27.54	28.00	29.45
$D_{rc}$ (cm)	20.00	20.00	20.02
$L$ (cm)	10.00	14.94	19.32
$n_s$	10	10	10
$l_m$ (mm)	11.40	6.40	5.50
$b_{ts}$ (mm)	3.00	5.40	4.00
$h_{ss}$ (mm)	12.70	20.00	25.10
$h_{sw}$ (mm)	4.20	2.00	4.30
$k_{open}$	0.9	0.2539	0.2004
$\delta$ (mm)	7.3	3.5	4

TABLE IV  
SPECIFICATION QUANTITIES VALUES THROUGH **FMINCON** OPTIMIZATION  
METHOD FOR INNER ROTOR GEOMETRY

	$CF_1$	$CF_2$	$CF_3$
Motor Total Weight ( $M_w^{tot}$ ) [kg]	62.30	80.04	111.00
Efficiency ( $\eta$ ) [%]	79.20	86.40	76.50
Magnets Total Weight ( $M_m^{tot}$ ) [kg]	4.24	5.47	3.04

TABLE V  
SPECIFICATION QUANTITIES VALUES THROUGH **GA** OPTIMIZATION  
METHOD FOR INNER ROTOR GEOMETRY

	$CF_1$	$CF_2$	$CF_3$
Motor Total Weight ( $M_w^{tot}$ ) [kg]	62.86	86.37	113.00
Efficiency ( $\eta$ ) [%]	79.10	82.1	74.80
Magnets Total Weight ( $M_m^{tot}$ ) [kg]	3.54	3.11	1.93

TABLE VI  
SPECIFICATION QUANTITIES VALUES THROUGH **PS** OPTIMIZATION  
METHOD FOR INNER ROTOR GEOMETRY

	$CF_1$	$CF_2$	$CF_3$
Motor Total Weight ( $M_w^{tot}$ ) [kg]	66.20	105.00	144.00

TABLE VII  
DESIGN VARIABLES RESULTS THROUGH **FMINCON** OPTIMIZATION  
METHOD FOR OUTER ROTOR GEOMETRY

	$CF_1$	$CF_2$	$CF_3$
$N_m$	72	58	46
$N_{spp}$	0.64	0.34	0.44
$D_o$ (cm)	24.91	42.18	25.10
$D_{rc}$ (cm)	24.00	25.31	23.60
$L$ (cm)	10.00	10.00	15.00
$n_s$	10	14	15
$l_m$ (mm)	8.80	7.10	5.00
$b_{ts}$ (mm)	2.50	3.70	8.80
$h_{ss}$ (mm)	6.00	14.30	10.00
$h_{sw}$ (mm)	1.00	1.00	4.70
$k_{open}$	0.90	0.233	0.89
$\delta$ (mm)	6.4	3.0	3.0

TABLE VIII  
DESIGN VARIABLES RESULTS THROUGH **GA** OPTIMIZATION METHOD FOR  
OUTER ROTOR GEOMETRY

	$CF_1$	$CF_2$	$CF_3$
$N_m$	60	78	60
$N_{spp}$	0.4722	0.1905	0.4772
$D_o$ (cm)	25.56	31.16	33.45
$D_{rc}$ (cm)	23.83	27.99	27.52
$L$ (cm)	10.00	10.01	10.00
$n_s$	13	10	10
$l_m$ (mm)	9.00	7.40	5.00
$b_{ts}$ (mm)	4.40	8.70	2.80
$h_{ss}$ (mm)	10.00	15.80	12.10
$h_{sw}$ (mm)	3.10	4.00	2.00
$k_{open}$	0.5748	0.2	0.6947
$\delta$ (mm)	4.2	3.0	9.1

TABLE IX  
DESIGN VARIABLES RESULTS THROUGH **PS** OPTIMIZATION METHOD FOR  
OUTER ROTOR GEOMETRY

	$CF_1$	$CF_2$	$CF_3$
$N_m$	26	46	26
$N_{spp}$	0.4351	0.48	0.6831
$D_o$ (cm)	31.30	34.48	37.77
$D_{rc}$ (cm)	29.12	32.85	35.06
$L$ (cm)	10.00	11.02	12.49
$n_s$	10	10	10
$l_m$ (mm)	14.30	10.80	6.40
$b_{ts}$ (mm)	17.30	7.80	9.90
$h_{ss}$ (mm)	14.60	10.80	13.50
$h_{sw}$ (mm)	4.70	4.00	4.70
$k_{open}$	0.9	0.3147	0.9
$\delta$ (mm)	14.4	4.2	15.2

TABLE X  
SPECIFICATION QUANTITIES VALUES THROUGH **FMINCON** OPTIMIZATION  
METHOD FOR OUTER ROTOR GEOMETRY

	$CF_1$	$CF_2$	$CF_3$
Motor Total Weight ( $M_w^{tot}$ ) [kg]	58.50	130.24	85.67
Efficiency ( $\eta$ ) [%]	79.77	89.05	78.06
Magnets Total Weight ( $M_m^{tot}$ ) [kg]	4.58	3.06	2.39

TABLE XI  
SPECIFICATION QUANTITIES VALUES THROUGH **GA** OPTIMIZATION  
METHOD FOR OUTER ROTOR GEOMETRY

	$CF_1$	$CF_2$	$CF_3$
Motor Total Weight ( $M_w^{tot}$ ) [kg]	58.12	82.30	72.25
Efficiency ( $\eta$ ) [%]	80.63	87.56	76.38
Magnets Total Weight ( $M_m^{tot}$ ) [kg]	4.10	5.24	2.41

TABLE XII  
SPECIFICATION QUANTITIES VALUES THROUGH **PS** OPTIMIZATION  
METHOD FOR OUTER ROTOR GEOMETRY

	$CF_1$	$CF_2$	$CF_3$
Motor Total Weight ( $M_w^{tot}$ ) [kg]	61.80	123.00	138.00

### C. Results & Discussion

The algorithms adopted applied in the PMSM motor design problem. Fig. 5 depicts the generic flowchart followed towards the optimization procedure. Tables I-III show the twelve design variables optimization results for the inner rotor geometry through the "fmincon", GA and PS algorithms respectively and for each one of the cost functions applied ( $CF_1$ - $CF_3$ ), while Tables VII-IX show the same results for the outer rotor configuration. It is clear that all algorithms succeed to converge to a (sub)-optimum design solution satisfying the existing constraints. For example, the outer diameter of the motor is kept within satisfactory limits (24-42cm, with a 20-50cm constraint), while the machine length lies mainly in the 10-12cm region with a single case exception of 19cm (with a 10-50cm constraint). More compact information can be found in Tables IV-VI and Tables X-XII where the total motor weight, total magnets weight and motor efficiency, through the algorithms used and for every cost function, for inner and outer rotor geometries are shown respectively. Here, it seems that if the machine weight is of primary concern (first cost function), the outer rotor geometry is the choice, with the GA taking the lead by presenting a very light (~58kg) and efficient (~80%) motor, by keeping the magnet weight low enough (~4kg) as seen in Table XI. The second "winner" in this case is "fmincon" applied to the same geometry (Table X), while PS fail to present satisfactory results. The same conclusions are valid in the case where the magnets weight is of primary concern (third cost function). The overall magnets weight range is ~2-5.5kg. GA presents a solution with low magnet weight (2.4kg), satisfactory efficiency (~76.4%), while keeping the total machine weight low (~72kg) as shown in Table XI. The second alternative is given again by "fmincon" (Table X), while PS method present very heavy machines in this case. Tables XIII-XIV show the computational costs for the adopted and applied methods. Here, the first place goes to "fmincon" method performing solutions in the order of magnitude of 2 seconds for our problem. PS needs almost 2.5 times more computational time, while GA is the slowest optimization method with an almost 10 seconds response time. Furthermore, the thermal calculations involving slot current density for each one of the geometries, are summarized in Table XV. It is seen that 16 out of 18 of them can be realized as air-cooled machines, where only two outer rotor cases need force-cooling. Finally, a comparison has been made with results found in literature [8] where sequential quadratic programming (SQP) algorithm was used. Fig. 6 shows the variation of total machine weight as a function of magnets weight, while Fig. 7 depicts a comparison of the total machine weight variation as a function of copper losses (60 pole number). It is clearly seen than the "fmincon" algorithm present better performance than SQP.

### V. CONCLUSIONS

The design problem of a radial flux PMSM with inner

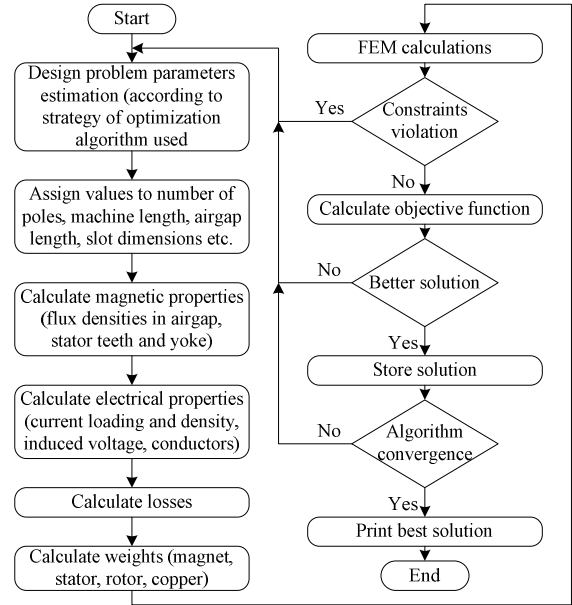


Fig 5. Algorithms' design optimization procedure flowchart.

TABLE XIII  
COMPUTATIONAL COST (SECS) OF OPTIMIZATION METHODS USED FOR INNER ROTOR GEOMETRY

	$CF_1$	$CF_2$	$CF_3$
<i>Fmincon</i>	2.241	2.604	2.012
<i>GA</i>	10.356	9.295	9.789
<i>Pattern Search</i>	5.476	5.299	5.286

TABLE XIV  
COMPUTATIONAL COST (SECS) OF OPTIMIZATION METHODS USED FOR OUTER ROTOR GEOMETRY

	$CF_1$	$CF_2$	$CF_3$
<i>Fmincon</i>	2.136	2.173	2.276
<i>GA</i>	9.596	8.115	9.112
<i>Pattern Search</i>	5.341	5.529	5.126

TABLE XV  
COMPUTED SLOT CURRENT DENSITY ( $A/cm^2$ ) OF ALL DESIGNS

	Inner Rotor			Outer Rotor		
	$CF_1$	$CF_2$	$CF_3$	$CF_1$	$CF_2$	$CF_3$
<i>fmincon</i>	690	534	315	873	820	608
<i>GA</i>	737	590	240	503	480	395
<i>PS</i>	800	577	223	583	569	551

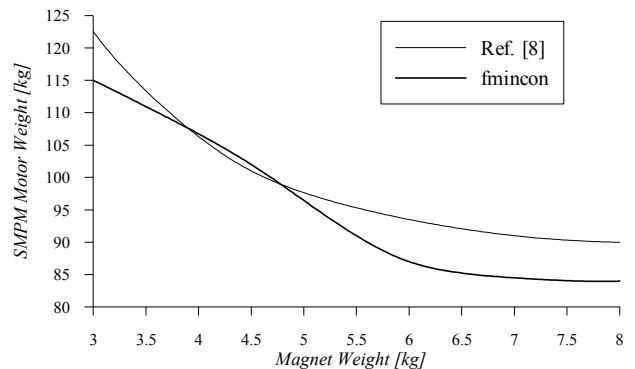


Fig 6. Variation of machine weight as a function of magnets weight.

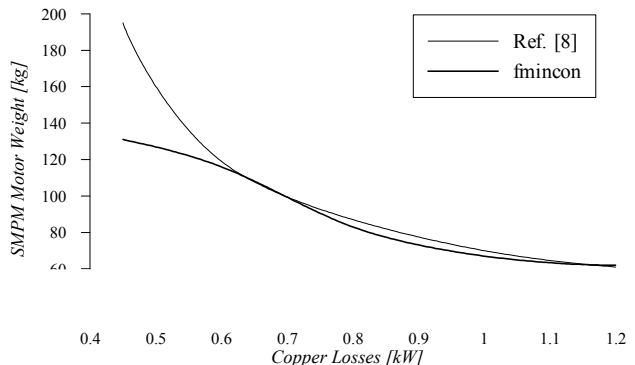


Fig 7. Variation of machine weight as a function of copper losses.

order to find competitive alternative designs to replace traditional low speed induction-motor/gearbox systems.

Fmincon, GA and PS were examined and an easily modified weighted objective function has been presented. An effort was made also to categorize and present briefly the large amount of data variables, constant and constraints needed in such a problem. The optimization results showed a stable convergence in solution sets of the 12 main problem variables. The most stable behavior was observed with "fmincon" method. Also, it was concluded that GA and "fmincon" methods are of priority compared to PS and SQP methods, if machine weight, magnets weight and computational time is of primary concern.

## VI. APPENDIX

TABLE XVI  
INDUCTION MOTOR-GEARBOX DATA CORRESPONDING TO PMSM

Quantity	Symbol	Unit	Ind. Motor	Gear-box	Total	PMSM
Outer Stator Dia.	$D_o$	cm	18	50	50	50
Machine length	$L$	cm	9.5	40.5	50	50
Machine Weight	$M_w^{tot}$	kg	22	131	153	150
Efficiency	$\eta$	%	88	90	79	79
Shaft Torque	$T$	Nm	28	1:30	840	840
Shaft Speed	$n$	rpm	1500	30:1	50	50
Output Power	$P_{out}$	kW	4.4	-	4.4	4.4
Line current	$I$	A	8.6	-	8.6	8.6
Supply voltage	$V_{LL}$	Volt	400	-	400	§II.D
Frequency	$f$	Hz	50	-	50	§II.D

TABLE XVII  
SEARCH DESIGN VARIABLES AND THEIR UNIVERSE OF DISCOURSE

Quantity	Symbol	Variable Range	Unit
No. of magnet poles	$N_m$	20 - 80	-
No. of slots / pole per phase	$N_{spp}$	0.001 - 1	-
Outer Stator Diameter	$D_o$	20 - 50	cm
Outer Rotor Diameter	$D_r$	$ 20 - D_o $	cm
Active machine length	$L$	10 - 50	cm
No. of parallel conductor paths	$n_s$	10 - 40	-
Magnet thickness	$l_m$	2 - 15	mm
Stator tooth width	$b_{ts}$	$\geq 2.5$	mm
Stator slot height	$h_{ss}$	$\geq 0$	mm
Slot wedge height	$h_{sw}$	1 - $h_{ss}$	mm
bs0/bss1 ratio	$k_{open}$	0.2 - 0.9	-
Airgap length	$\delta$	3 - 20	mm

TABLE XVIII  
CONSTANT VALUES INVOLVED IN THE DESIGN PROCEDURE

Quantity	Symbol	Set Value	Unit
Maximum flux density (NdFeB)	$B_{max}$	1.6	Tesla
Remanence flux density	$B_r$	1.08	-
Area occupied by conductors	$k_{cp}$	0.25	-
Operating frequency	$f$	50	Hz
Relative permeability	$m_r$	1.03	-
Motor's shaft speed	$n$	50	rpm
Mass density of the copper	$P_{copper}$	8920	kg/m <sup>3</sup>
No. of phases	$N_{ph}$	3	-
Mass density of the back iron	$P_{bi}$	7750	kg/m <sup>3</sup>
Copper resistivity	$\rho_{Cu}$	$1.72 \times 10^{-8}$	$\Omega/m$
Mass density of the magnet	$P_m$	7500	kg/m <sup>3</sup>
Torque on the motor's shaft	$T$	840	Nm

TABLE XIX.  
DESIGN PROBLEM CONSTRAINTS

Description	Symbol	Constraint
Stator yoke height	$h_{sy}$	$\geq h_{ss}/2$
Slot wedge height	$h_{sw}$	$\geq 1mm$
Slot opening height	$h_{s0}$	$\geq 2mm$
Slot width	$b_{ss2}$	$0.15h_{ss} \leq b_{ss2} \leq 0.5h_{ss}$
Tooth width	$b_{ts}$	$\geq 0.3\tau_s$
Slot opening width	$b_{ss0}$	$\geq 2mm$
Flux density in stator teeth	$B_{ts}$	$\leq 1.6T$
Flux density in stator yoke	$B_{sy}$	$\leq 1.4T$

Copper losses	$r_{Cu}$	$\sim 0.001$
Magnet weight	$M_m^{tot}$	$\leq 5.5kg$
Machine weight	$M_w^{tot}$	$\leq 150kg$

## VII. REFERENCES

- [1] P. Waide, C. Brunner, "Energy-Efficiency Policy Opportunities for Electric Motor-Driven Systems", International Energy Agency (IEA) Working Paper, Paris, France (www.iea.org), 2011.
- [2] E. Spooner, A.C. Williamson, "Direct coupled, permanent magnet generators for wind turbine applications", *IEEE Proceedings - Electric Power Applications*, vol. 143, no. 1, January 1996, pp. 1-8.
- [3] M.R.J. Dubois, "Optimized Permanent Magnet Generator Topologies for Direct-Drive Wind Turbines", *Doctoral Thesis*, TU Delft, Delft University of Technology, 2004.
- [4] J.Y. Chen, C.V. Nayar, X. Longya, "Design and finite-element analysis of an outer-rotor permanent-magnet generator for directly coupled wind turbines", *IEEE Trans. on Magnetics*, vol. 36, no. 5, 2000, pp. 3802-3809.
- [5] Ø. Krøvel, R. Nilssen, S.E. Skaar, E. Løvli, N. Sandøy, "Design of an Integrated 100kW Permanent Magnet Synchronous Machine in a Prototype Thruster for Ship Propulsion", in *Proc. of the 16<sup>th</sup> Int. Conference on Electrical Machines (ICEM' 04)*, Cracow, Poland, Sep. 5-8, 2004, cd.ref. 697.
- [6] R. Fichoux, F. Caricchi, F. Crescimbeni, H. Onorato, "Axial-flux permanent-magnet motor for direct-drive elevator systems without machine room", *IEEE Transactions on Industry Applications*, vol. 37, no. 6, 2001, pp. 1693-1701.
- [7] F. Meier, "Permanent-Magnet Synchronous Machines with Non-Overlapping Concentrated Windings for Low-Speed Direct-Drive Applications", *Doctoral Thesis*, Royal Institute of Technology, KTH, Stockholm, 2008.
- [8] F. Libert, J. Soulard, "Design Study of a Direct-Driven Surface Mounted Permanent Magnet Motor for Low Speed Application", in *Proc. of the 5th International Symposium on Advanced Electromechanical Motion Systems - ELECTROMOTION 2003*, vol. 1, Marrakesh, Morocco, November 26-28, 2003.
- [9] J. Pyrhonen, T. Jokinen, V. Hrabovcova, *Design of Rotating Electrical Machines*, 2nd Ed., John Wiley & Sons, 2013.
- [10] F. Magnussen, C. Sadarangani, "Winding factors and Joule losses of permanent magnet machines with concentrated windings", in *Proc of IEEE International Electric Machines & Drives Conference (IEMDC)*, Madison, Wisconsin, June 2003, pp. 333-339.
- [11] D.G. Dorell, "Combined thermal and electromagnetic analysis of permanent-magnet and induction machines to aid calculation", *IEEE Trans. on Industr. Electronics*, vol. 55, no. 10, 2008, pp.3566-3574.
- [12] J. R. Hendershot, T.J.E. Miller, "Design of Brushless Permanent Magnet Machines", 2<sup>nd</sup> ed., Motor Design Books LLC, 2010.
- [13] Optimizations Toolbox™ User's Guide, Matlab Release R2013b, The Mathworks Inc, MA, USA, 2013.
- [14] G. Mitsuo, C. Runwei, *Genetic Algorithms and Engineering Optimization*, John Wiley & Sons, Canada, 2000.
- [15] A.E. Eiben, P-E. Raué, "Genetic algorithms with multi-parent recombination", in *Proc. of the 3rd Conference on Parallel Problem Solving from Nature*, LNCS 866, Springer-Verlag, 1994, pp.78-87.
- [16] C. Audet, J.E. Dennis Jr. "Analysis of Generalized Pattern Searches." *SIAM Journal on Optimization*, vol. 13, no. 3, 2003, pp. 889-903.
- [17] ITT Flygt, Product catalogue, Mixing products section (low speed), (www.flygt.com).

## VIII. BIOGRAPHIES

**Yannis L. Karnavas** was born in Volos, Hellas, 1969. He is with the Electrical Machines Laboratory at the Dept. of Electrical & Computer Engineering, Democritus University of Thrace, Xanthi, Hellas, as an Assistant Professor. His research interests include electrical machines design, analysis and modeling, design and application of electrical machines controllers and artificial intelligence methods application to them. He has published several papers in various national, international journals and conferences as well as book chapters in international engineering books. He has participated in research projects as research leader or scientific associate. He serves as an Associate Editor and as an Editorial board member in various international scientific journals. He is an IEEE member.

**Christos D. Korkas** graduated from the Department of Electrical and Computer Engineering, Democritus University of Thrace, Xanthi, Hellas, where he is currently pursuing his PhD degree. His research interests lie in the energy management area. Since October 2013 he has been involved in

